Journal of Materials Chemistry C

Accepted Manuscript

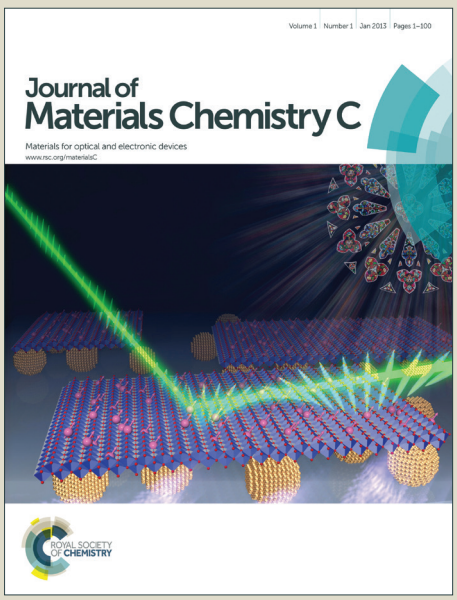

ROYAL SOCIETY OF CHEMISTRY

www.rsc.org/materialsC

Journal of Materials Chemistry C

RSCPublishing

ARTICLE

In-situ Photo-Induced Chemical Doping of Solution-Processed Graphene Oxide for Electronic Applications

Cite this: DOI: 10.1039/x0xx00000x

Received 00th January 2012,
Accepted 00th January 2012

DOI: 10.1039/x0xx00000x

www.rsc.org/

K. Savva,[a] A. Y-H. Lin[b], C. Petridis[c,d], E. Kymakis[d], T.D. Anthopoulos[b,*] and E. Stratakis[a,e,*]

We developed a photochemical method for the simultaneous reduction and doping of graphene oxide (GO) layers through ultraviolet laser irradiation in the presence of a dopant precursor gas. It is shown that a few seconds of irradiation is sufficient to dope the GO lattice, while the doping and reduction levels can be readily controlled upon variation of the irradiation time. Using this method, the simultaneous reduction and doping of GO with chlorine or nitrogen atoms is achieved and confirmed by Raman, FTIR and X-ray photoelectron (XPS) spectroscopy measurements. To demonstrate the potential of the approach for practical applications, the photochemical method was successfully employed for the in-situ laser induced modification of prefabricated GO field effect transistors. Real time monitoring of the evolution of charge transport as a function of irradiation time reveals significant changes, a result attributed to the chemical modification of the GO lattice. The facile, rapid and room temperature nature of the photo-induced method proposed here provides unique opportunities for the cost-effective synthesis of bulk amounts of chemically modified GO for a wide range of applications spanning from transistors and sensors to transparent electrodes for lighting and photovoltaic cells.

Introduction

Graphene is a 2-dimensional (2D), zero band gap material with unique morphological, mechanical, optical, thermal and electrical properties[1,2]. However, the majority of graphene's applications are handicapped by the absence of a semiconducting band gap. As a result, numerous methods have been developed to introduce dopants into graphene's lattice and in this way to engineer its band gap[3,4,5,6,7,8,9,10,11,12]. One alternative method to dope graphene involves the chemical functionalization of graphene oxide (GO) lattice[13,14,15,16,17,18,19] – a route that could potentially provide access to novel and previously unexplored graphene derivatives. Unfortunately, most of the methods reported to date fail to demonstrate precise control over doping levels and exhibit poor yield or scalability, posing limits for practical applications. In addition, the high temperatures processes often required are time-consuming but, more importantly, are not compatible with emerging temperature-sensitive technologies such as large-area plastic/printed electronics. Therefore the development of a simple, low-temperature and high-throughput method for controllable doping of graphene is highly desirable.

Here we report a novel, facile and room temperature methodology that can be used for controllable photochemical doping of GO. GO contains large numbers of functional oxygen groups (e.g. epoxy, hydroxyl, carboxyl, carbonyl) that could potentially be exploited in order to photo-chemically tune its electrical properties. A successful photochemical event is realized by the light-induced partial removal of such functional groups and the subsequent insertion of hetero-atoms into the GO lattice[20,21]. To date, various laser irradiation approaches have been adopted for GO treatment and are reviewed in Ref. 22. Of great interest is the laser induced reduction of the GO lattice[23] demonstrated to be suitable for the realization of flexible graphene electrodes[24] and tailoring of the GO bandgap[25]. Moreover lasers had been used for the in-situ treatment of GO devices[26]. Finally, a recently published work[27] showed that femtosecond laser irradiation can been used for N doping of GO. Our method relies on precise photochemical reactions initiated by a pulsed laser irradiation in the presence of a dopant precursor gas. It is rapid and efficient since a few nanosecond pulses are sufficient to induce doping levels of a few percent. By simple tuning of the laser parameters the exact doping level can be controlled with good reproducibility. The technique negates the need for high temperatures post deposition steps and can provide access to the synthesis of large quantities of doped graphene sheets with good control over the doping level, which is not readily realized by existing methods. Using this method, the simultaneous reduction and doping of

GO with a few percent of chlorine or nitrogen atoms was realized following irradiation in the presence of Cl_2 or NH_3 gases, respectively. We show that upon photochemical doping chlorine and nitrogen atoms substitute GO defects located on the edges as well as in the plane of the GO lattice[9,11,28]. To demonstrate the applicability of the method for practical device applications we study the electronic properties of pristine and photo-chemically doped GO layers using field-effect transistors (FET) measurements.

Experimental

GO layers fabrication

Graphite oxide was synthesized by the modified Hummers method and exfoliated to give a brown dispersion of GO under ultrasonication. The resulting GO was negatively charged over a wide pH condition, as the GO sheet had chemical functional groups of carboxylic acids. GO solution in ethanol (0.5 mg/ml) at pH 3.3 was dropped after an oxygen plasma treatment for 2 min in order to make the ITO surface hydrophilic. The GO solution was maintained for a waiting period of 2 min and was then spun at 3000 rpm for 30 s, followed by 30 min baking at 100 °C inside a nitrogen-filled glove box. The thickness of the films was analogous to the number of spinning repetitions; a film thickness of 3.4 nm was obtained with two successive coatings.

Photochemical doping of GO films

The as-spun GO layers on Si or PET substrates were subjected to irradiation by a KrF excimer laser source emitting 20 ns pulses of 248 nm at 1Hz repetition rate that was translated onto the film area. For uniform exposure of the whole sample to laser radiation, a top-flat beam profile of 20×10 mm^2 was obtained using a beam homogenizer. The whole process took place into a vacuum chamber at 50 Torr Cl_2 or NH_3 gas pressure maintained through a precision micro valve system. Different combinations of laser powers (P) and number of pulses (N_p) were tested in an effort to optimize the photochemical functionalization processes. In a typical experiment, the sample was irradiated at a constant P with N_p = 10, 20, 30, 40, 50, 60, 120, 600 and 1200, corresponding to different photochemical reaction times.

Field effect transistors (FETs) fabrication

Bottom-gate, bottom-contact FETs were initially prepared using pristine GO sheets. The transistors structures were fabricated using heavily doped p-type Si wafers acting as a common back-gate electrode and a 200 nm thermally grown SiO_2 layer as the gate dielectric. Using conventional photolithography, the gold source-drain (S-D) electrodes were defined with channel lengths and widths in the range 1-40 µm and 1-20 mm, respectively.

Microscopic and Spectroscopic Characterization

The morphology of the film surfaces was examined by atomic force microscopy (AFM; Digital Instruments NanoScope IIIa). (Supporting Information, Figure S1) Fourier transform infrared (FTIR) spectra were measured on a BRUKER FTIR spectrometer IFS 66v/F (MIR). Raman spectroscopy was performed using a Nicolet Almega XR Raman spectrometer (Thermo Scientific) with a 473 nm blue laser as an excitation source. X-ray photoelectron spectroscopy (XPS) measurements were carried out in a Specs LHS-10 Ultrahigh Vacuum (UHV) system. The XPS spectra were recorded at room temperature using unmonochromatized AlKa radiation under conditions optimized for maximum signal (constant ΔE mode with pass energy of 36 eV giving a full width at half maximum (FWHM) of 0.9 eV for the Au 4f7/2 peak). The analyzed area was an ellipsoid with dimensions 2.5 x 4.5 mm^2. The XPS core level spectra were analyzed using a fitting routine, which allows the decomposition of each spectrum into individual mixed Gaussian-Lorentzian components after a Shirley background subtraction. The ultraviolet photoelectron spectroscopy (UPS) spectra were obtained using HeI irradiation with hν = 21.23 eV produced by a UV source (model UVS 10/35). During UPS measurements the analyzer was working at the Constant Retarding Ratio (CRR) mode, with CRR = 10. The work function was determined from the UPS spectra by subtracting their width (i.e. the energy difference between the analyzer Fermi level and the high binding energy cutoff), from the HeI excitation energy. For these measurements a bias of −12.30 V was applied to the sample in order to avoid interference of the spectrometer threshold in the UPS spectra. All the work function values obtained by UPS were calibrated with scanning kelvin probe microscopy (SKPM) measurements. The relative error is 0.02 eV.

Results and Discussion

The GO starting material used here was synthesized by a modified Hummers' method[29]. The GO water dispersion was then spin coated directly onto Silicon or PET[24] substrates.

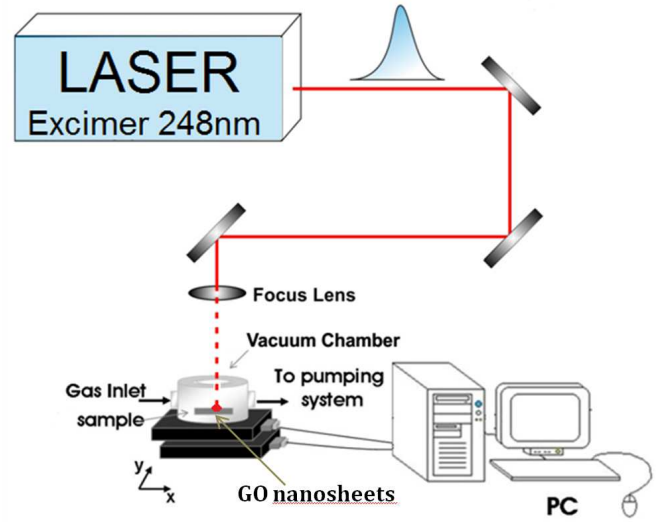

Figure 1: Schematic of the experimental set-up used for the laser-induced doping of GO nanosheets.

Figure 1 presents the irradiation scheme used for the realization of the doping process. The as-spun GO layers were subjected to irradiation by a KrF excimer laser source emitting 20 ns pulses of 248 nm at 1Hz repetition rate that was translated onto the film area. For uniform exposure of the whole sample to laser radiation, a top-flat beam profile of 20×10 mm^2 was obtained using a beam homogenizer. The whole process took place into a vacuum chamber at 50 Torr Cl_2 or NH_3 gas pressure maintained through a precision micro valve system. Different combinations of laser powers (P) and number of pulses (Np), were tested in an effort to optimize the photochemical functionalization processes. In a typical experiment, the sample was irradiated at a constant P=25mW with Np = 10, 20, 30, 40, 50, 60, 120, 600 and 1200, corresponding to different photochemical reaction

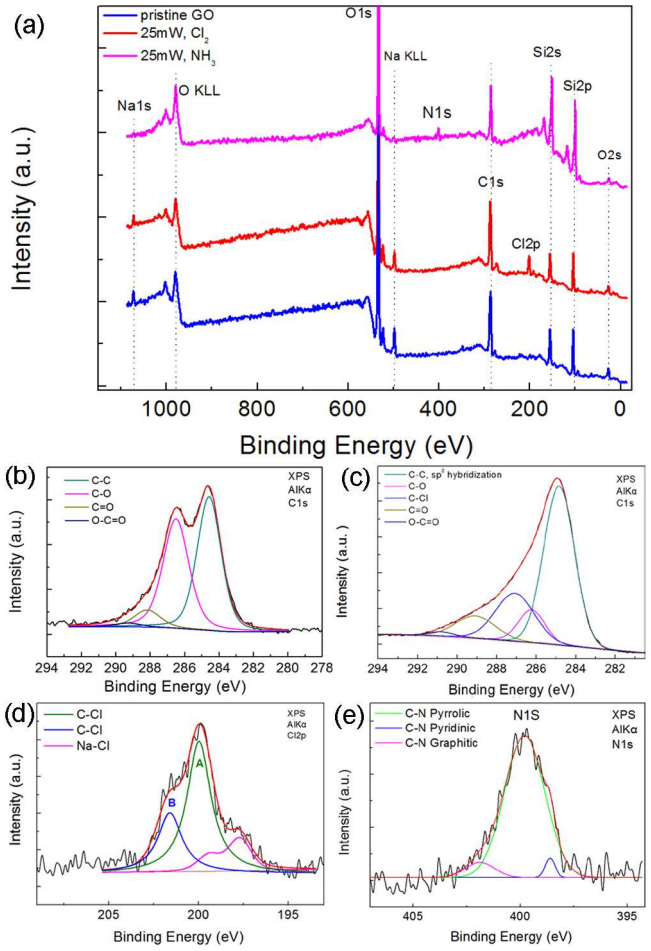

Figure 2: (a) XPS survey spectra of pristine and laser treated GO in Cl_2 and NH_3; high-resolution XPS C1s spectra of GO in its pristine (b), and laser treated in Cl_2 (c) state; d) high resolution Cl2p XPS spectra of GO-Cl layers; high resolution N1s XPS spectra of GO-N layers.

times. It should be noted here that the results are similar with those obtained upon irradiation with different intensities. Following irradiation, X-ray photoelectron spectroscopy (XPS) was used to probe and quantify the level of dopants introduced into the GO lattice. The respective measurements were carried out using a Kratos Axis Ultra spectrometer with Al Ka monochromated X-ray beam at low pressures. Figure 2a compares typical spectra of the pristine and Cl-doped GO. From this data it can be seen that the intensity of the O1s peak relative to that of C1s is reduced while the characteristic Cl2p appears after irradiation. These results indicate a laser-induced simultaneous reduction and Cl doping of the GO sheets. The Na peaks visible in the XPS scans are contributions from the sample mounting procedure and can therefore be ignored.

Analysis of the core level characteristic peaks allowed insight to be gained into the nature of the chemical bonds in each case. Figures 2b-c present in high resolution the respective C1s and Cl2p peaks showing that, after irradiation, the C-O/C-C intensity ratio decreases from 1.09 to 0.60 while the Cl2p/C1s intensity ratio becomes equal to 0.17. In particular, the C1s spectrum of as-prepared GO sheets showed a second peak at higher binding energies, corresponding to large amounts of sp^3 carbon with C-O bonds, carbonyls (C=O), and carboxylates (O-C=O)[30], resulted from harsh oxidation and destruction of the sp^2 atomic structure of graphene.

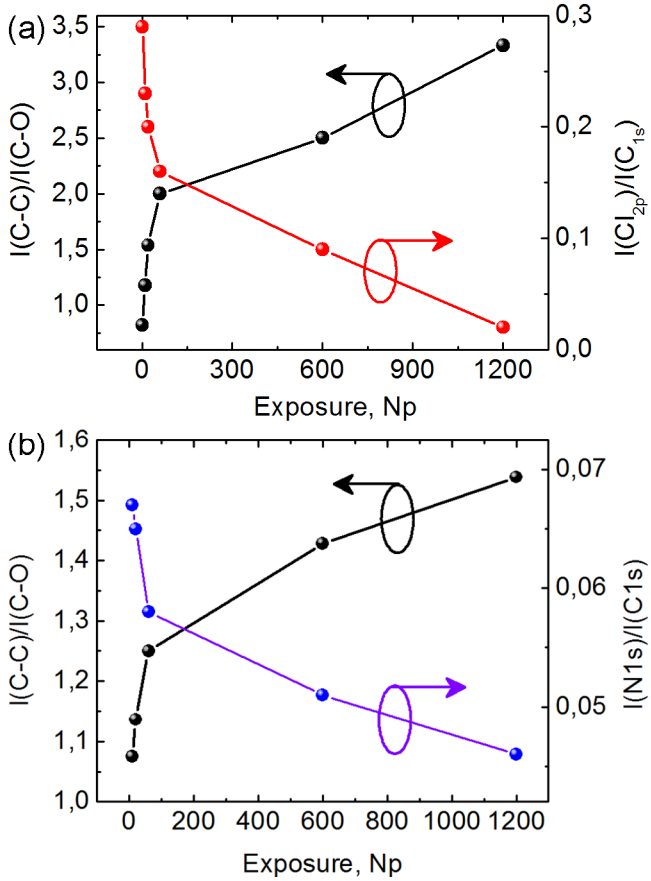

Figure 3: a) GO reduction and Cl doping levels as a function of number of laser pulses, N_p; b) GO reduction and Cl doping levels as a function of number of laser pulses, N_p;

In our technique, by carefully tuning key laser parameters, the Cl-doping level could be readily controlled. Increase of P in the range from 10 to 50 mW or increase of N_p at a certain P, give rise to a corresponding decrease of the doping level. As shown in Figure 3a, there is a rapid decrease of the Cl2p/Cls ratio upon

increasing N_p while at the same time a sharp increase in the GO reduction degree is evident. The maximum introduction of Cl-groups attained was ~11.3 atom % as can be estimated by the ratio of the Cl2p to the C1s peak areas after considering the atomic sensitivity factors for Cl2p and C1s. We investigated the bonding configurations of Cl atoms in laser treated GO sheets based on high-resolution Cl2p XPS spectra; a typical example is presented in Figure 2d. In all cases, the Cl2p peaks could be fitted into two peaks, one of lower energy, A ($2p_{3/2}$) and one of higher, B ($2p_{1/2}$). In all the samples, peak A was close to 200 eV and peak B near 201.7 eV corresponding to Cl–C at the edges and Cl–C=O groups, respectively[31]. The above findings indicate enhancement of the doping efficiency upon increasing the number of the GO oxygen groups, suggesting that Cl-doping most likely occurs at the edges and defect sites[32,33]

Similar results have been acquired using NH_3 gas as a precursor doping agent. The corresponding high resolution N1S peak of Figure 2e depicts that the nitrogen groups present in the N-doped graphene comprises a pyridinic (at ~398.6 eV), a pyrrolic (at ~399.8 eV) and a quaternary or graphitic nitrogen (at ~401.8 eV) peaks[16]. Earlier work attributed these contributions to the regions of pyridinic or pyrrolic peaks to the presence of amine groups[15,16]. The corresponding dependence of N-doping level on N_p is presented in Figure 3b. As in the case of Cl-doping oxygen groups existing at the edges and defect sites in the plane of GO react with NH_3, giving rise to N-doping, readily detected by XPS spectroscopy. The simultaneous reduction and N-doping of the GO nanolayers treated in NH_3 had been also confirmed via FTIR measurements (Supporting information, Figure S1). Following irradiation, the C=O and C-OH vibrational peaks were significantly reduced, while two characteristic new bands appeared at 1030 cm^{-1} and 1650 cm^{-1} due to the C-N bond stretch vibrations[34] and the bending mode of amide bonds[35] respectively.

Raman spectroscopy, one of the most sensitive techniques for the investigation of carbon based materials[32], has been also used to investigate the effect of laser irradiation on the reduction and doping of the GO nanosheets. Figure 4a depicts the respective spectra before and after laser irradiation in the presence of Cl_2. All spectra show the two prominent D (at ~1330 cm^{-1}) and G (at ~1590 cm^{-1}) bands, associated with carbon-based materials, corresponding to the degree of disorder and graphitization respectively[36,37]. Also, the presence of a weak 2D band is typical for chemically derived graphene. Although this band was not altered appreciably with the exposure time, the D and G bands were observed to change upon increasing the number of laser pulses, as shown in the inset of Figure 4a. In particular, the intensity ratio of the D to G bands (I_D/I_G), which is commonly used as a measure of defect levels in graphene, is seen to progressively increase with exposure time (I_D/I_G ~ 0.88 before laser treatment and 0.95 after (Figure 4b). It had been found that, an increase of I_D/I_G ratio in GO indicates lattice disordering or ordering depending on the starting defect levels. Based on the measured decrease in channel conductance of the laser-doped GO transistors presented below the increase of I_D/I_G ratio can be attributed to an increase in defects and disorder in laser treated samples, associated with the decrease in the sp^2-C content as well as the presence of the Cl–C=O form. Furthermore, both peaks gradually shift to higher wavenumbers upon increasing the number of pulses, with the G peak shifting by ~10 cm^{-1}, while the D by ~4 cm^{-1} (Supporting information, Figure S2). The observed blue shift of the G-band position has been attributed to phonon stiffening with doping of GO[38,39]. Moreover, as shown in Figure 4c, the G band becomes narrower while at the same time the D band gets broader with increasing exposure time. The D line broadening complies with the I_D/I_G ratio increase and can be attributed to enhancement of GO reactivity as more defect sites are created[40]. On the other hand, the G band narrowing may be attributed to the doping effect suggesting that covalent bonds C – Cl bonds were formed and thus a transformation of the sp^2 type C-C bonds to sp^3 had been induced[9]. The saturation effect observed for I_D/I_G, G and D peaks position and FWHM after illumination with 60 pulses complies with the trend of saturation in doping efficiency observed in the respective XPS spectra (i.e. compare Figures 2 and 4). Based on the above XPS and Raman analysis, it can be concluded that the reduction and doping levels can be readily controlled by increasing the laser exposure time. Most important, XPS measurements reveal that the laser induced dopants are stable for months upon sample storage in ambient conditions.

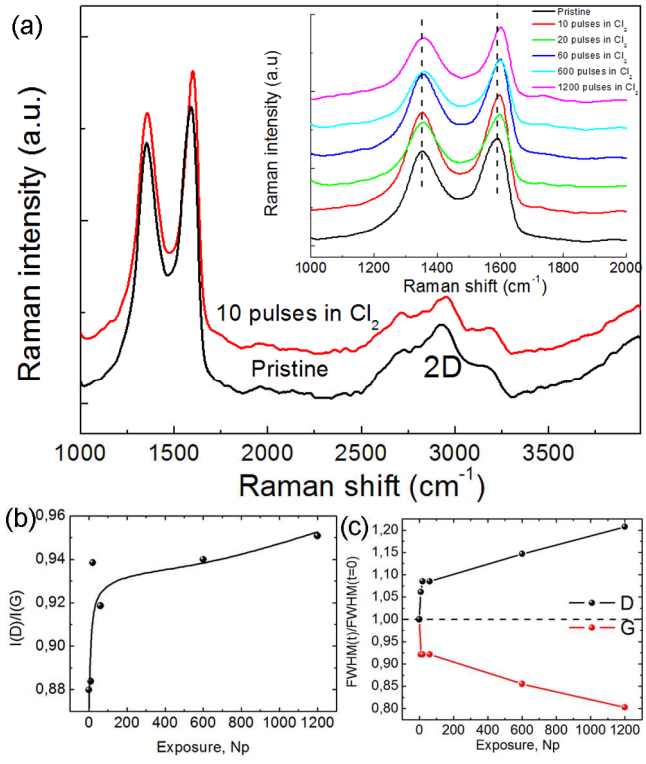

Figure 4: (a) Micro-Raman measurements of GO sheets before (pristine) and after irradiation with 10 laser pulses in Cl_2; the evolution of the G and D bands with different number of pulses is presented in the inset; (b) Dependence of the I_D/I_G ratio on the number of the laser pulses, N_p; (c) Dependence of the D and G bands FWHM (normalized values) on N_p

Concerning the mechanism behind laser-induced doping, it can be postulated that upon excitation with UV laser pulses, chlorine and nitrogen radicals are generated in the gas phase via photodissociation of Cl_2 and NH_3 precursor gases respectively[41]. Subsequenlty, the radicals formed preferentially react with the GO lattice via, thermodynamically favorable, free radical addition reactions[11,21]. At the same time, electrons generated under irradiation can be captured by GO hence leading to GO reduction[42]. Further investigations are currently in progress to explore and understand the exact mechanism behind the laser-induced doping process.

To investigate how N- and Cl- doping affects the microscopic electronic properties of graphene, bottom-gate, bottom-contact FETs were initially prepared using pristine GO sheets. The transistors structures were fabricated using heavily doped p-type Si wafers acting as a common back-gate electrode and a 200 nm thermally grown SiO_2 layer as the gate dielectric (Figure 5a-b). Using conventional photolithography, the gold source-drain (S-D) electrodes were defined with channel lengths and widths in the range 1-40 µm and 1-20 mm, respectively. The GO flakes were deposited by dip-coating at room-temperature directly onto 1.5 cm × 1.5 cm size substrates containing few hundreds of pre-patterned S-D electrode pairs. The samples were then thermally annealed at 200 °C in nitrogen. As-prepared devices were subjected to in-situ laser irradiation under identical conditions used for the experiments performed on nanolayers.

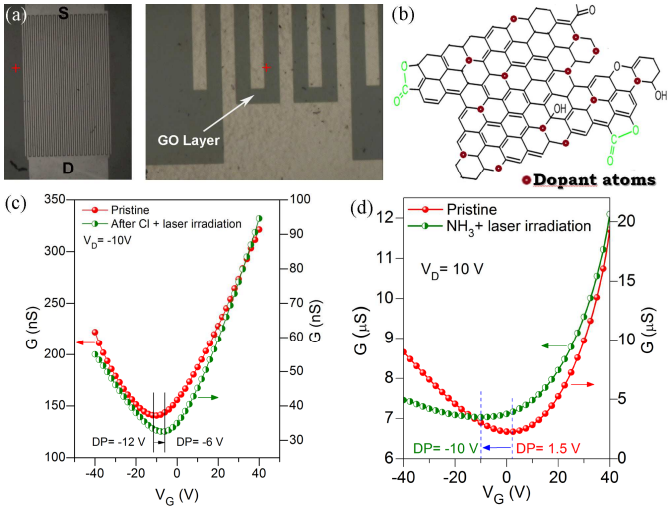

Figure 5: (a) Optical microscopy images of GO FETs; (b) Schematic representation of reduced and doped GO lattice; (c) Transfer characteristics measured for FETs based on rGO before (pristine) and after exposure of the channel to Cl and laser irradiation (Cl_2 + laser irradiation); (e) Transfer characteristics measured for FETs based on rGO before (pristine) and after exposure of the channel to NH_3 and laser irradiation (NH_3 + laser irradiation).

Figures 5c-d shows the channel transconductances (G) versus gate voltage (V_G) characteristics for two GO transistors before and after laser irradiation in the presence of Cl_2 and NH_3 gases, respectively. For the annealed GO devices (pristine) the G–V_G plot shows the typical 'V' shaped ambipolar transfer characteristic[7] with a distinct asymmetry in the electron and hole branches. The charge neutrality point (CNP) for the pristine GO devices was found to vary between 2 V to -12 V. The often measured positive values for the DP indicate unintentional p-doping, probably caused by oxygen species physisorbed on the surface/edges of the GO layers during device preparation[28]. In order to study the impact of laser irradiation in the presence of different dopant gases on the transport properties of GO channels, the transfer curves for each device were recorded prior to and after laser irradiation with and without the dopant gas present. To ensure the validity of the changes in the transfer curves following the doping process, the laser treatment was performed in-situ in postfabricated transistors. In a typical experiment the pristine transfer curve of a transistor based on undoped GO was recorded followed by laser treatment in the presence of the dopant precursor gas. Afterwards, the new transfer curve was measured and compared to that obtained in the pristine state. In the time periods among the measurements, the transistor was kept into inert atmosphere in order to avoid unintentional doping due to physisorbed atoms and molecules.

Laser treatment in the presence Cl_2 gas leads to a drop in the overall channel conductance under both p- and n-channel operation. The clear shift in the CNP to more positive voltages is most likely the result of the enhanced p-type conductivity of the GO channel due to the photochemically induced p-type doping of GO[7,43]. This observation is in qualitative agreement with the shift in the work function (WF) of the GO layer from 4.91 eV to 5.23 eV measured before and after laser irradiation, respectively (Supporting information, Figure S3-a). Laser irradiation of the control samples under inert atmosphere is found to have no distinguishable impact on the transporting characteristics of the device (Supporting information, Figure S3b). Based on these results we conclude that the observed changes in the channel conductance can only be attributed to p-doping caused primarily by laser induced photoreaction with the dopant gas (Cl_2).

Sample	μ_{lin} [cm^2/Vs]		I_{ON}/I_{OFF}	
	Before Irradiation	After Irradiation	Before Irradiation	After Irradiation
Laser treated in NH_3 (50 mJ, 10 pulses)	3.10×10^{-3}	9.83×10^{-4}	2.25	8.91
Laser treated in Cl_2 (50 mJ, 10 pulses)	16.3×10^{-3}	3.81×10^{-3}	1.53	3.61

Table 1: Carrier mobilities and on/off ratios of GO transistors subjected to laser treatment in Cl_2 and NH_3 respectively.

When the GO channel was irradiated with laser light in the presence of NH_3 (Figure 5d), the device characteristics exhibit the opposite trend to that seen in transistors irradiated in the presence of Cl_2 gas (Figure 5c). In particular, the CNP is found

to shift to more negative gate voltages indicative of n-type doping[44]. This observation is in good agreement with the measured shift in the WF function from 4.91 eV for the pristine GO to 4.6 eV for laser irradiated GO in the presence of NH_3 (Supporting information, Figure S3-b). Table I summarizes the respective on/off ratios and mobility values for GO transistors treated in Cl_2 and NH_3 respectively. It is clear that the photochemical process is rapid, since a few nanosecond pulses in the presence of a reactive dopant gas are sufficient to induce up to a five-fold increase of the channel on/off ratio[9]. In contrast to the WFs changes described above, the relatively small change of the on/off ratio indicates a minor electronic effect due to dopant atoms.

The general decrease in GO conductivity (holes and electrons) observed upon photochemical doping suggests an increase in the structural disorder in agreement with the Raman measurements presented above. Such lattice disorder could be caused either by interruption of the conjugated system or the introduction of scattering centers[45,46]. The decrease in both electron and hole mobilities together with the G-band narrowing are indications that the laser induced photochemical reaction(s) gives rise to substitutional doping at the expense of surface charge transfer doping[9]. This observation is in contrast to the increase in carrier mobility and improvement in the lattice order observed upon laser treatment of GO under inert atmosphere[26]. The present results confirm that laser irradiation of GO under inert atmosphere does not induce any structural disorder and the presence of reactive dopant gas(es) combined with laser irradiation is the main reason for the observed doping effects.

Conclusions

Based on the results presented here it can be concluded that laser irradiation in the presence of a reactive gas can be used as an easy and catalyst-free approach for the synthesis of doped GO derivatives. The proposed method is simple and offers access to controllable reduction and doping of GO at room temperature hence allowing combination of the technique with temperature sensitive substrate materials such as plastic. The rather simple and scalable method could potentially be used for the synthesis of novel graphene-based derivatives that are difficult or impossible to obtain via conventional synthetic routes.

Acknowledgements

This work was supported by the Integrated Initiative of European Laser Research Infrastructures LASERLAB-III (Grant Agreement No. 2012-284464). The authors acknowledge Ms. Labrini Syggelou for her support with the XPS/UPS measurements.

Notes and references

[a] Institute of Electronic Structure and Laser (IESL), Foundation for Research and Technology – Hellas (FORTH), Heraklion, 71003, Greece.
[b] Department of Physics & Centre for Plastic Electronics, Imperial College London, Blackett Laboratory, London SW7 2BW, United Kingdom.
[c] Department of Electronic Engineering, TEI of Crete, Chania 73132, Crete, Greece.
[d] Center of Materials Technology and Photonics & Electrical Engineering Department, Technological Educational Institute (TEI) of Crete, Heraklion, 71003, Greece.
[e] Materials Science and Technology Department, University of Crete, Heraklion, 71003, Greece
[*] Corresponding authors

1 K.S. Novoselov, A.K. Geim, S.V. Morozov, D. Jiang, Y. Zhang, S.V. Dubonos, I.V. Grigorieva and A.A. Firsov, *Science*, 2004, **306**, 666 - 669
2 A. Geim and K.S. Novoselov, *Nat. Mater.*, 2009, **324**, 1530 - 1534
3 S. Yu, W. Zheng, C. Wang and Q. Jiang, *ACS Nano*, 2010, **4**, 7619 - 7629
4 F. Schedin, A.K. Geim, S.V. Morozov, E.W. Hill, P. Blake, M.I. Katsnelson and K.S. Novoselov, *Nat. Mater.*, 2007, **6**, pp. 652 – 655
5 C. Casiraghi, *Physical Review B*, **80**, 2009, pp. 233407
6 B. Guo, L. Fang, B. Zhang, J.R. Gong, *In sciences Journal*, 2011, **1**, pp. 80-89
7 Z. Luo, N. J. Pinto, Y. Davila and A.T.C. Johnson, *Appl. Phys. Lett.*, 2012, **100**, pp. 253108-1 – 253108-4.
8 E. Bekyarova, M.E. Itkis, P. Ramesh, C. Berger, M. Spinkle, W.A. de Heer and R.C. Haddon, *J. Am. Chem. Soc.*,, 2009, **131**, pp. 1336
9 H. Liu, Y. Liu and D. Zhu, *J. Mater. Chem.*, 2011, **21**, pp.3335 – 3345
10 D.C. Elias, R.R. Nair, T.M.G. Mohiuddin, S.V. Morozov, P. Blake, M.P. Halsall, A.C. Ferrari, D.W. Boukhvalov, M.I. Katsnelson and A.K. Geim, *Science*, 2009, **323**, pp. 610 – 613
11 B. Li, L. Zhou, D. Wu, H. Pang, K. Yan, Y. Zhou and Z. Liu, *ACS Nano*, 2011, **5**, pp. 5957 – 5961.
12 L. Zhang, S. Diao, Y. Nie, K. Yan, N. Liu, B. Dai, Q. Xie, A. Riena, J. Kong, Z. Liu, *JACS*, 2011,**133**, pp. 2706 – 2713
13 L. Zhang, Y. Ye, D. Cheng, W. Zhang, H.Pan and J. Zhu, *Carbon*, 2013, **62**, pp. 365 – 373.
14 Peiwei Gong, Zhaofeng Wang, Zhangpeng Li, Yongju Mi, Jinfeng Sun, Lengyuan Niu, Honggang Wang Jinqing Wang and Shengrong Yang, *RSC Advances*, 2013, **3**, pp 6327
15 X. Li, H. Wang, J.T. Robinson, H. Sanchez, G. Diankov and H. Dai, *J. Am. Chem. Soc.*, 2009, **131**, pp. 15939 – 15944
16 Nanjundan Ashok Kumar, H. Nolan, N.McEvoy, E. Reznavi, R. Doyle, M. Lyons and G. Duesberg, *J. Mater. Chem. A*, 2013, **1**, pp. 4431-4435
17 Tran Ngoc Huan, Tran Van Khai, Youngjong Kang, Kwang Bo Shimb and Hoeil Chung, *J. Mater. Chem.*, 2012, **22**, pp 14756-14762
18 Y. Liu, N. Tang, X. Wan, Q. Feng, M. Li, Q. Xu, F. Liu and Y. Du, *Scientific Reports*, 2013 **3**, Article number: 2566

19 Gulbagh Singh, D S Sutar, V Divakar Botcha, Pavan K Narayanam, S S Talwar, R S Srinivasa and S S Major, *Nanotechnology*, 2013, **24**, 355704
20 S. Wang, P.J. Chia, L.L. Chua, L.H. Zhao, R.Q. Png, S. Sivaramakrishnan, M. Zhou, R.G.S. Goh and R.H. Friend, *Adv. Mater*., 2008, **20**, 3440
21 H. Liu, S. Ryu, Z. Chen, M.L. Steigerwald, C. Nuckolls and L. E. Brus, *J. Am. Chem. Soc.*, 2009, **131**, pp. 17099 – 17101.
22 Y.-L. Zhang, L. Guo, H. Xia, Q.-D. Chen, J. Feng, H.-B. Sun, *Adv. Opt. Mater.* 2014, **2**, 10.
23 Y. Zhang, L. Guo, S. Wei, Y. Hec, H. Xia, Q. Chen, H.-B. Sun, F.-S. Xiao, *Nano Today*, 2010, **5**, 15.
24 E. Kymakis, K. Savva, M.M. Stylianakis, C. Fotakis and E. Stratakis, *Adv. Funct. Mat.*, 2013, **23,** pp. 2742-2749
25 L. Guo, R.-Q. Shao, Y.-L. Zhang, H.-B. Jiang, X.-B. Li, S.-Y. Xie, B.-B. Xu, Q.-D. Chen, J.-F. Song, H.-B Sun, *J. Phys. Chem. C*, 2012, **116**, 3594.
26 C. Petridis, Y-H Lin, K. Savva, G. Eda, E. Kymakis, T.D. Anthopoulos and E. Stratakis, *Appl. Phys. Lett*, 2013, **102**, pp 093115.
27 L. Guo , Y.-L. Zhang, D.-D. Han, H.-B. Jiang, D. Wang, X.-B. Li, H. Xia, J. Feng, Q.-D. Chen, H.-B. Sun, *Adv. Opt. Mater*. 2014, **2**, 120.
28 T.O. Wehling, K.S. Novoselov, S.V. Morozov, E.E. Vdovin, M.I. Katsnelson, A.K. Geim and A.I. Lichnenstein, *Nano Letters*, 2008, **8**, pp. 173 – 177
29 Z. Luo, Y. Lu, L. A. Somers and A. T. C. Johnson, *J. Am. Chem. Soc*., 2009, **131**, pp. 898-899
30 S. Stankovich, D. A. Dikin, R. D. Piner, K. A. Kohlhaas, A. Kleinhammes, Y. Y. Jia, Y. Wu, S. T Nguyen, R. S. Ruoff, *Carbon*, 2007, **45**, pp. 1558–1565
31 D.-W. Wang , K.-H. Wu , I. R. Gentle, G. Q. Lu, *Carbon*, 2012, **50**, pp. 333
32 X. Wang, X. Li, L. Zhang, Y. Yoon, P.K. Weber, H. Wang, J. Guo and H. Dai, *Science*, 2009, **324**, pp. 768 – 771
33 J. L. Bahr, J. P. Yang, D. V. Kosynkin, M. J. Bronikowski, R. E. Smalley and J.M. Tour, , *J. Am. Chem. Soc.*, 2001, **123**, pp. 6536 – 6542
34 T. Ramanathan, F. T. Fisher, R. S. Ruoff, and L. C. Brinson *Chem. Mater*. , 2005, **17**, pp. 1290
35 N. Karousis, S. P. Economopoulos, E. Sarantopoulou, N, Tagmatarchis, *Carbon*, 2010, **48**, pp. 854
36 A. C. Ferrari, *Solid State Commun*., 2007, **143**, pp. 47-57
37 D. Zhan, ZH Ni, W. Chen, L. Sun, ZQ Luo, LF Lai, *Carbon* 2011, **49**, pp 1362-6
38 M. A. Pimenta , G. Dresselhaus , M. S. Dresselhaus , L. G. Cancado, A. Jorio , R. Saito , *Phys. Chem. Chem. Phys*. 2007 , **9** , pp. 1276
39 A. Das, S. Pisana, B. Chakraborty, S. Piscanec, S. K. Saha , U. V. Waghmare, K. S. Novoselov, H. R. Krishnamurthy, A. K. Geim, A. C. Ferrari, A. K. Sood, *Nat. Nanotechnol*. 2008, **3**, pp. 210
40 H. Liu, S. Ryu, Z. Chen, M.L. steigerwald, C. Nuckolls, L. E. Brus, *J. Am. Chem. Soc*.,, 2009, **131**, pp. 17099 – 17101
41 Hiroyasu Sato, *Chem. Rev.* 2001, **101**, pp. 2687-2726
42 Y. Matsumoto, M. Koinuma, S. Ida, S. Hayami, T. Taniguchi, K. Hatakeyama, H. Tateishi, Y. Watanabe and S. Amano, *J. Phys. Chem. C*, 2011, **115**, pp. 19280–19286
43 Goki Eda, Yun-Yue Lin, Steve Miller, Chun-Wei Chen, Wei-Fang Su and Manish Chhowalla, *Appl. Phys. Lett*. 2008, **92**, pp. 233305
44 Yung-Chang Lin, Chih-Yueh Lin and Po-Wen Chiu, *Appl. Phys. Lett*., 2010, **96**, pp. 133110
45 G. Eda, A. Nathan, P. Wobkenberg, F. Colleaux, K. Ghaffarzadeh, T. Anthopoulos and M. Chhowalla, *Appl. Phys. Lett.*, 2013, **102**, pp. 133108
46 D.C. Elias, R.R. Nair, T.M. Mohiuddin, S.V. Morozov, P. Blake, M.P. Halsall, A.C. Ferrari, D.W. Bouchvalov, M.I. Katsnelson, A.K. Geim, K.S. Novoselov, *Science*, 2009, **323**, pp. 610 – 613